

Resonance attractors of spiral waves in excitable media under global feedback

Vladimir S. Zykov and Harald Engel

Institut für Theoretische Physik, Technische Universität Berlin, Hardenbergstrasse 36, D-10623 Berlin, Germany

(Received 13 February 2002; published 12 July 2002)

The dynamics of spiral waves on a circular domain is studied by numerical integration of an excitable reaction-diffusion system with a global feedback. A theory based on the Fourier expansion of the feedback signal is developed to explain the existence and the stability of resonance attractors of spiral waves on domains of different sizes. The theoretical analysis predicts the existence of a discrete set of stable attractors with radii depending on the time delay in the feedback loop. These predictions are in good quantitative agreement with performed numerical simulations.

DOI: 10.1103/PhysRevE.66.016206

PACS number(s): 05.45.-a, 05.65.+b, 82.40.Bj, 47.54.+r

I. INTRODUCTION

Spiral waves subjected to parametric forcing exhibit very rich spatiotemporal dynamics. Apart from a pure theoretical interest, the controlled motion of spiral waves induced by a parametric modulation of the excitability is important for many applications, e.g., for the defibrillation of cardiac tissue [1–3]. The resonance attractor gives an example of such unusual spiral wave dynamics that is intensively studied now [4–9].

The existence of the resonance attractor is closely connected to the resonance drift of spiral waves induced by a parametric forcing of an excitable medium at a frequency exactly equal to the eigenfrequency of the spiral wave [10–12]. Such a drift provides an efficient way to control the location of a spiral wave within a restricted domain of an excitable medium and allows one even to push it toward the boundary of the medium, when it is necessary to stop self-sustained activity [2,8,10].

The resonance attractor has been discovered in excitable systems under a feedback control, when a pulsatory modulation of the excitability was synchronized with the passage of the wave fronts through a measuring point that can be arbitrarily chosen in the medium [4]. This feedback forcing induces a drift of the spiral core along a circular pathway centered at the measuring point. The theory of the resonance attractor under pulsatory modulation reduces the dynamics of a spiral wave under one-channel feedback to a low dimensional iterative map [6,9]. It predicts the existence of circular orbits and quantitatively describes their sizes. Recent experimental studies [8,9] reveal a complex structure of the attractor in that circular orbits of different radii coexist, depending on the sign and the time delay in the feedback loop.

Another possibility to synchronize parametric forcing with the intrinsic dynamics is to apply a global feedback. Such a feedback has been effectively used in order to induce clustering and wave instabilities in oscillatory active media [13], to suppress chaotic oscillation [14] or to stabilize and/or destabilize a spiral wave in an excitable medium [15].

In the first part of this work we describe our numerical results illustrating the existence of the resonance attractor of spiral waves in a circular domain of an excitable medium under a global feedback. Then a theory is developed to describe the dynamics of spiral waves under such a control.

The existence and the stability of the attractor orbits are analyzed. Finally, the obtained theoretical predictions are compared with numerical data.

II. MATHEMATICAL MODEL

In our computations, a general two-component mathematical model is used to describe excitable media in terms of “reaction-diffusion” equations

$$\frac{\partial u}{\partial t} = D_u \nabla^2 u + F(u, v) - I(t), \quad (1)$$

$$\frac{\partial v}{\partial t} = D_v \nabla^2 v + \epsilon G(u, v),$$

where variables $u(x, y, t)$ and $v(x, y, t)$ (sometimes called activator and inhibitor) can be interpreted as the concentrations of the reagents involved in a hypothetical chemical reaction taking place in a thin (quasi-two-dimensional) layer. Function $I(t)$ specifies the parametric forcing [e.g., illumination of the light-sensitive Belousov-Zhabotinsky (BZ) solution] applied uniformly to the whole domain.

For the functions $F(u, v)$ and $G(u, v)$, we took the form earlier used in Ref. [15],

$$\begin{aligned} F(u, v) &= f(u) - v, \\ f(u) &= -k_1 u, \quad u \leq \sigma, \\ &= k_f(u - a), \quad \sigma < u < 10 - \sigma, \\ &= k_2(10 - u), \quad 10 - \sigma \leq u, \end{aligned} \quad (2)$$

$$\begin{aligned} G(u, v) &= k_g u - v, \quad k_g u - v \geq 0, \\ &= k_\epsilon(k_g u - v), \quad k_g u - v < 0 \end{aligned}$$

with the following parameter values: $k_f = 1.7, k_g = 2, k_\epsilon = 6.0, a = 0.1, \sigma = 0.01, \epsilon = 0.3, D_u = 1, D_v = 0$. The parameters k_1 and k_2 are chosen in such a way that the function $f(u)$ is continuous at $u = \sigma$ and $u = 10 - \sigma$.

The system (1) was integrated for a circular domain of radius R_d with the time step $\Delta t = 0.02$ and the space step $h = 0.4$. Dirichlet boundary conditions have been chosen:

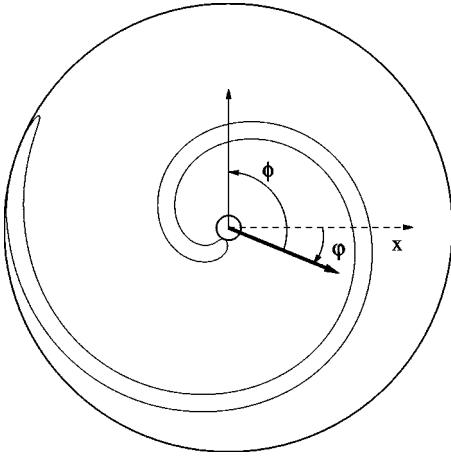


FIG. 1. Spiral wave rigidly rotating in a circular domain of radius $R=96=1.5\lambda$ described by the system (1) with $I(t)=0$ and Dirichlet boundary conditions. The computed value of the integral B is $B_0=1.0$. Contour line $v(x,y,t)=2.0$ is shown at the instant $t=t_0$. Direction of the induced drift under parametric forcing with $I(t)=0.02\cos[2\pi(t-t_0)/T-\phi]$ is shown by thick (thin) arrow for $\phi=0$ ($\phi=0.6\pi$).

$u|_{R_d}=v|_{R_d}=0$ in contrast to no-flux conditions used in Ref. [15]. Dirichlet conditions better approximate the experimental situation, for instance, when a circular-shaped piece of a gel layer with immobilized catalyst is placed in the BZ solution.

For an autonomous system with $I(t)=0$ this model has a steady state $u=v=0$ that is stable with respect to a small perturbation. However, a superthreshold perturbation, once locally applied, gives rise to a wave propagating through the medium. Moreover, by a special choice of initial conditions a rigidly rotating spiral wave can be created as shown in Fig. 1. The measured period of this rotation is $T=51.3$ and the spiral pitch is $\lambda=64.0$. The spiral wave tip describes a circular pathway of radius $R_q=5.87=0.092\lambda$.

To introduce a global coupling the feedback signal $I(t)$ is computed as

$$I(t)=k_{fb}[B(t-\tau)-B_0], \quad (3)$$

where

$$B(t)=\frac{1}{S}\int_S v(x,y,t)dx dy. \quad (4)$$

Thus, the intensity of the feedback signal is proportional to the integral value B of the second variable over the simulated domain S . Two important control parameters in the feedback loop are the gain k_{fb} and the time delay τ . Note that in the case of a rigid rotation of a spiral wave exactly around the domain center, integral B does not depend on time. The constant B_0 in Eq. (3) is the value of this integral. Hence, the application of such a feedback does not change the parameters of the rigid rotation, since the feedback signal vanishes for this case.

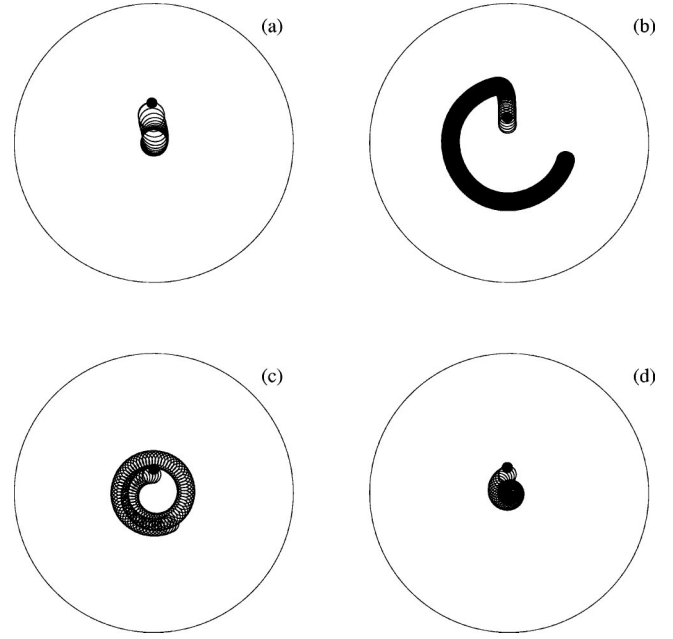


FIG. 2. Trajectories of a spiral wave tip in the model (1) subjected to the global feedback with the gain $k_{fb}=0.1$. The initial location of the spiral wave tip at $t=0$ is shown by the black dot. In (a) the spiral core motion is stabilized at the center of the circular domain of radius $R_d=\lambda$ ($\tau=0, 0\leq t\leq 1000$). In (b) and (c) $R_d=1.5\lambda$. In (b) and (c) the centrally symmetric rotation is unstable and the core motion approaches a resonance attractor with radius depending on the time delay: (b) $\tau=0, 0\leq t\leq 30\,000$, (c) $\tau=14, 0\leq t\leq 5000$. In (d) $\tau=18, 0\leq t\leq 5000$ and the attractor radius vanishes.

III. COMPUTATIONS UNDER GLOBAL COUPLING

It is known that in an autonomous system such as Eq. (1) with $I(t)=0$ the parameters of a rigidly rotating spiral wave do not depend on the applied boundary conditions until the distance from the spiral core center to the boundary is large enough [16]. Due to this property a spiral wave slightly displaced with respect to the domain center will continue to circulate with the same rotation period around a core of the same radius. In this case the computed integral B should be a periodic function of time. If the feedback loop is closed, the feedback signal should disturb the rigid rotation inducing the resonant drift.

Figure 2(a) shows the trajectory of the spiral wave tip computed for a circular domain of radius $R_d=\lambda$ with positive gain $k_{fb}=0.1$ in the feedback loop and $\tau=0$. The initial location of the core center was shifted in the positive y direction by $\Delta y=0.15\lambda$. After two revolutions of the spiral, the feedback loop was closed that induced a drift of the core toward the domain center until the trajectory is completely stabilized and started to circulate around the domain center. The feedback signal corresponding to this dynamical process is shown in Fig. 3(a). At the beginning of the process the signal oscillates with a relatively large amplitude that vanishes with time while the spiral core approaches the domain center. Remaining small amplitude (about $0.01k_{fb}B_0$) oscillations occur with the period $T/4$ and are induced by the applied discretization scheme where diagonal directions are

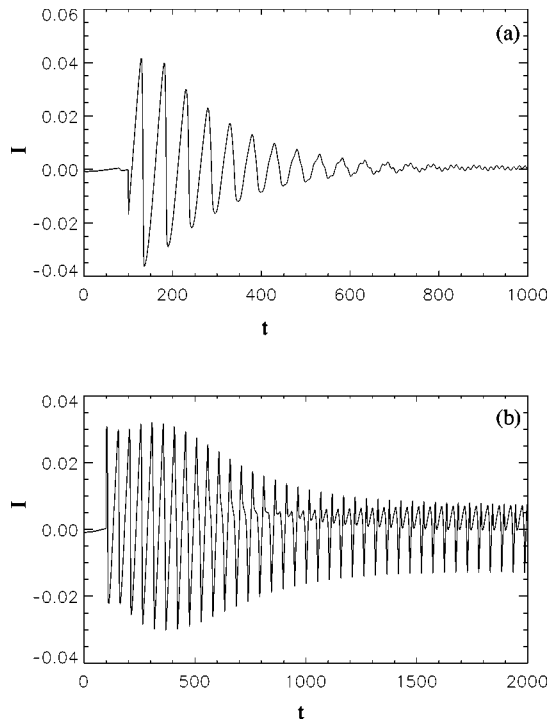


FIG. 3. Feedback signal $I(t)$ computed from Eqs. (3) and (4) for the trajectories shown in Figs. 2(a) and 2(b), correspondingly.

not identical to the x and/or y directions.

It is very important to compare this result with similar computations performed for the domain radius $R_d = 1.5\lambda$ as shown in Fig. 2(b). In contrast to the previous case, the spiral core starts to drift and a radial component of this motion is directed from the domain center. In the course of time, the velocity of this radial motion becomes smaller. Finally, it vanishes and a pure azimuthal drift remains. Thus the core center trajectory approaches a circular pathway that looks very similar to the resonance attractor recently observed in the case of the one-channel feedback generating a pulsatory feedback signal [6,8]. In our computations the feedback signal is a smooth function of time oscillating with the rotation period T of the spiral wave, as shown in Fig. 3(b). The amplitude and the complex shape of these oscillations remain constant during the motion of the core along the resonance attractor.

The radius of the observed resonance attractor can be controlled by variation of the time delay τ in the feedback loop. For instance, in Fig. 2(c) a tip trajectory computed with $\tau = 14$ is shown. In these computations the same initial conditions as in the previous case have been used. However, the core center moves finally along an orbit of smaller radius.

Moreover, by increasing the time delay, the attractor radius can be reduced to zero. An example of such an attractor is shown in Fig. 2(d). When this attractor is approached, the rigid rotation of the spiral wave around the domain center is established, as in the case shown in Fig. 2(a). Thus, by an appropriate choice of the time delay it is possible to induce a stabilization of a spiral wave, shown in Fig. 2(d), or its destabilization, shown in Fig. 2(b).

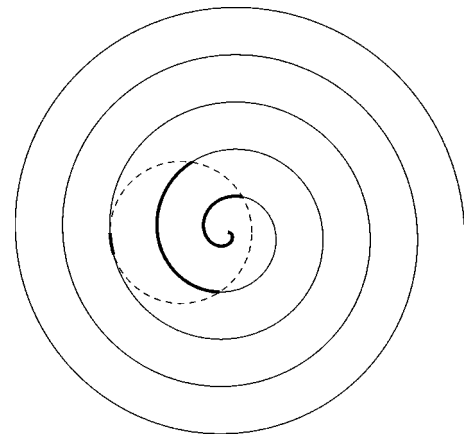


FIG. 4. Archimedean spiral given by Eq. (5) (solid line) shifted with respect to the domain center of radius $R_d = 1.5\lambda$ (dashed line). The segments of the spiral located within the domain (thick solid line) give input into the integral $B(t)$. Displacement $d = \lambda$.

Note that the recently elaborated theory of the resonance attractor under one-channel feedback [6,9] cannot be applied in order to explain the phenomena observed in our computations, since it deals with pulsatory feedback signals and reduces the spiral dynamics to a low dimensional iterative map. In the considered case of a global coupling, the feedback signal is a continuous function of time and to describe the observed spiral wave dynamics a new theoretical approach should be developed.

IV. ARCHIMEDIAN SPIRAL APPROXIMATION

Figure 3(b) demonstrates that the motion of the spiral wave core in our computations is induced by a periodic parametric forcing of the system. Although the modulation function $I(t)$ has been computed during simulation of a system with a feedback, exactly the same drift trajectory will be obtained if $I(t)$ is treated as an *a priori* given function of time. Of course, the same initial and boundary conditions should be applied in order to reproduce the drift trajectory.

It is clear that the computed value of the feedback signal depends on the spiral shape and the location of the spiral wave core. Let us assume that the induced drift is so slow that the shape and the angular velocity of the rotating spiral remain always the same. Then our aim is to estimate the computed feedback signal for a given location of the spiral wave core.

An appropriate approximation for the observed feedback signal can be based on the following assumption. First note that the spiral wave shown in Fig. 1 is rather thin, which is a common feature of waves in low excitable media. Hence the integral B should be proportional to the arc length L of the spiral wave front: $B = bL/S$, where b is a positive constant. Second, the shape of the front can be approximated by an Archimedean spiral [17,18].

Under these assumptions the estimation of the integral B is reduced to a pure geometrical problem: It is necessary to calculate the arc length of an Archimedean spiral within a circular domain of a given radius, as illustrated in Fig. 4.

Counterclockwise rotation of the spiral displaced in the positive x direction on a distance d will induce periodic variations of the arc length within the domain. To evaluate these variations, it is easier to assume that the domain center is displaced in the negative x direction on the distance d and rotates clockwise around the core center of the motionless spiral.

Let an Archimedian spiral be specified in a polar coordinate system (r, Θ) by an equation

$$\Theta = \Theta_0 - \frac{2\pi}{\lambda} r, \quad (5)$$

where λ is the spiral pitch and the spiral is oriented in such a way that $\Theta_0 = 0$. It is easy to see that if $d < \lambda$ there is only one intersection point between the spiral and the domain boundary. Let (r_p, Θ_p) and (x_p, y_p) be the coordinates of the intersection point in the polar and Cartesian coordinate system, respectively. They should obey the following system of algebraic equations:

$$\Theta_p = -\frac{2\pi}{\lambda} r_p, \quad (6)$$

$$R_d^2 = (x_p - \Delta x)^2 + (y_p - \Delta y)^2, \quad (7)$$

$$x_p = r_p \cos \Theta_p, \quad (8)$$

$$y_p = r_p \sin \Theta_p. \quad (9)$$

Here, $(\Delta x, \Delta y)$ are the coordinates of the domain center. In accordance with our assumptions, the center rotates clockwise around the origin of the coordinate system, that gives

$$\begin{aligned} \Delta x &= d \cos \alpha, \\ \Delta y &= d \sin \alpha, \\ \alpha &= -\pi - \omega t, \end{aligned} \quad (10)$$

where $\omega = 2\pi/T$ is the rotation frequency of the spiral.

After simple transformations the following equation for r_p can be derived:

$$r_p^2 + d^2 - 2r_p d \cos(\Theta_p - \alpha) = R_d^2. \quad (11)$$

An analytical solution for this equation can be found in the limit $d \ll \lambda/2 < R_d$. Indeed, for such a small shift d Eq. (11) can be reduced to

$$r_p^2 - 2r_p d \cos(\Theta_d - \alpha) = R_d^2, \quad (12)$$

where $\Theta_d = -2\pi R_d/\lambda$. A solution for this equation under the assumption $d \ll R_d$ can be written in the form

$$r_p = R_d + d \cos(\Theta_d - \alpha). \quad (13)$$

Thus, the value r_p oscillates near R_d with the frequency ω . Substituting this solution into Eq. (6), variations of the angle Θ_p can be expressed as

$$\Theta_p = \Theta_d - \frac{2\pi}{\lambda} d \cos(\Theta_d - \alpha). \quad (14)$$

If $R_d > \lambda/2$, deviations of the arc length L of the spiral inside the circular domain can be considered to be proportional to deviations of Θ_p ,

$$L = L_0 - R_d(\Theta_p - \Theta_d) = L_0 + \frac{2\pi d R_d}{\lambda} \cos(\Theta_d - \alpha). \quad (15)$$

Due to proportionality between L and B an expression for the integral B can be written in the following form:

$$B(t) = B_0 + \frac{2db}{R_d \lambda} \cos\left(\omega t + \pi - \frac{2\pi}{\lambda} R_d\right). \quad (16)$$

Thus, if the shape of a spiral wave is close to an Archimedian one and if its displacement from the domain center is small ($d \ll \lambda/2 < R_d$), Eq. (16) shows that the feedback signal should be a harmonic function of time with a phase depending on the domain radius R_d . This result is important for stability analysis of a centrally symmetric rotation.

V. STABILITY OF THE CENTRALLY SYMMETRIC ROTATING SPIRAL

A periodic parametric forcing induces a resonant drift of the spiral wave core, as was shown analytically [19,20], and convincingly demonstrated in experiments [5,10,12] and computations [21–23]. The direction of the drift, of course, depends on the initial orientation of a spiral and on the parameters of the excitable medium [19]. In our computations the direction of the induced drift for the spiral located at $t = 0$ as shown in Fig. 1 occurs in the direction of the thick arrow, if the periodic forcing has the form $I(t) = A \cos(\omega t)$. The calculated drift is specified by the angle $\varphi = -0.1\pi$.

The direction of the drift depends also on the phase of an external forcing. It is obvious that under external forcing $I(t) = A \cos(\omega t - \phi)$ the direction of the induced drift will be turned by the angle ϕ , as illustrated in Fig. 1 for $\phi = 0.6\pi$.

It is important to note that the front of the spiral wave shown in Fig. 1 can be approximated by an Archimedian spiral given by Eq. (5) with $\Theta_0 = 0$, since at the radial distance $R_d = 1.5\lambda$ (i.e., at the domain boundary) the polar angle has the value $\Theta = -\pi$. Hence, this spiral has the same orientation as an Archimedian spiral described by Eq. (6), applied to derived Eq. (16).

Let us apply these properties of the induced drift in order to analyze the stability of the centrally symmetric rotation of a spiral wave with respect to a small radial shift. To this aim assume that the spiral wave shown in Fig. 1 is displaced in the positive x direction. From Eqs. (3) and (16) it follows that due to this displacement an external parametric forcing will appear in the form

$$I(t) = k_{fb} \frac{2db}{R_d \lambda} \cos\left(\omega t - \omega \tau + \pi - \frac{2\pi}{\lambda} R_d\right). \quad (17)$$

Substitution of $R_d=1.5\lambda$ and $\tau=0$ into Eq. (17) gives

$$I(t)=k_{fb}\frac{2db}{R_d\lambda}\cos(\omega t). \quad (18)$$

Thus, in this case the phase shift ϕ is equal to zero. It means that after a small displacement in the positive x direction the computed feedback signal will force the spiral wave to drift in the direction of the thick arrow in Fig. 1.

It is very important to stress that the direction of the drift induced by the global feedback does not depend on the initial orientation of a displaced spiral. A reason for this is that the phase of the external forcing determined by Eq. (17) is also dependent on the initial orientation, in contrast to the case of an *a priori* given modulation law. If the initial orientation of the spiral is turned by an angle $\Theta_0 \neq 0$ with respect to the orientation shown in Fig. 1, a phase of the $I(t)$ in Eq. (17) should be also changed by Θ_0 . As a result, in accordance with the properties of a resonant drift mentioned before, the direction of an induced drift will remain the same as it was at $\Theta_0=0$.

Moreover, it becomes clear that the direction of a drift induced by the global feedback after an arbitrary oriented small displacement will be turned by the angle φ with respect to the direction of this displacement. Hence, an evolution of a radial and an azimuthal component of the core displacement (R_c, Θ_c) can be expressed in the following form:

$$\frac{dR_c}{dt}=V\cos\gamma, \quad (19)$$

$$\frac{d\Theta_c}{dt}=\frac{V}{R_c}\sin\gamma, \quad (20)$$

where V is an absolute value of the drift velocity and the angle γ determines the drift direction. In accordance with Eq. (17) and our computations shown in Fig. 1, the angle γ corresponding to a small displacement d is determined by the following expression:

$$\gamma=\varphi+\omega\tau-\pi+\frac{2\pi}{\lambda}R_d. \quad (21)$$

In the case shown in Fig. 2(b), where $\tau=0$ and $R_d=1.5\lambda$, the angle γ can be written as $\gamma=\varphi+2\pi$. Of course, an additional turn by 2π does not change the real direction of the induced drift shown by the thick arrow in Fig. 1. The initial displacement will grow since $-\pi/2 < \varphi < \pi/2$ and, hence, the derivative dR_c/dt determined by Eq. (19) is positive. That corresponds to the unstable regime shown in Fig. 2(b).

However, if the time delay in the feedback loop is sufficiently large, the induced drift can be directed toward the domain center that should reduce the initial displacement and produce a stabilization of the centrally symmetric rotation. A corresponding condition for the time delay can be derived from Eqs. (19) and (21) taking into account that for stability the derivative dR_c/dt should be negative. Then the stability

condition for the centrally symmetric rotation in a domain of radius $R_d=1.5\lambda$ can be written as

$$0.5\pi+2\pi m-\varphi < \omega\tau < 1.5\pi+2\pi m-\varphi, \quad (22)$$

where m is an arbitrary integer. An example of such stabilization computed with $\omega\tau=0.72\pi$ is shown in Fig. 2(d).

Equations (19) and (21) show that the stability conditions depend on the domain radius R_d . Indeed, substituting $R_d=\lambda$ and $\tau=0$ into Eq. (21) we get

$$\gamma=\varphi+\pi. \quad (23)$$

Hence, in this case the direction of an induced drift should be turned by the angle $\phi=\pi$ with respect to the thick arrow in Fig. 1. Obviously, such a drift will cause a decrease of the initial displacement and a stabilization of the centrally symmetric rotation in accordance with our calculation shown in Fig. 2(a). This consideration allows us to generalize the stability condition (22) for the case of an arbitrary value of the domain radius that gives

$$0.5\pi+2\pi m-\varphi < \omega\tau-\pi+\frac{2\pi}{\lambda}R_d < 1.5\pi+2\pi m-\varphi. \quad (24)$$

The centrally symmetric rotation of a spiral wave is stable with respect to a small radial shift if the conditions (24) are valid for an integer number m .

It is important to stress that the stability conditions (24) can be applied only in the case of a positive gain k_{fb} in the feedback loop. Application of a negative gain should be equivalent to an additional phase shift equal to π . Hence, for a negative gain the stability conditions are

$$-0.5\pi+2\pi m-\varphi < \omega\tau-\pi+\frac{2\pi}{\lambda}R_d < 0.5\pi+2\pi m-\varphi. \quad (25)$$

Note that under a monotonous increase of the domain size stability and instability of the centrally symmetric rotation alternate periodically. Indeed, if the rigid rotation of a spiral wave is stable in a domain of radius $R_d=\lambda$, this regime will be stable for all domains with radii $R_d=n\lambda$, and will be unstable for $R_d=1.5\lambda+n\lambda$. Here n is an integer number.

A similar periodicity takes place with respect to the time delay τ . If the domain size is fixed and for a given τ_s a stabilization occurs, then it will be observed also for $\tau=\tau_s+nT$, while for $\tau=\tau_s+0.5T+nT$ a destabilization will take place.

VI. EXISTENCE AND STABILITY OF THE RESONANCE ATTRACTOR

Computation of the resonance attractor as illustrated in Fig. 2(b) shows that the induced drift in this case occurs also due to a periodic parametric forcing of the system [see Fig. 3(b)]. The core center of a spiral wave moves along this attractor of radius R_a . A displacement d of the core with respect to the domain center is exactly equal to the attractor radius R_a and cannot be considered as a small parameter. In

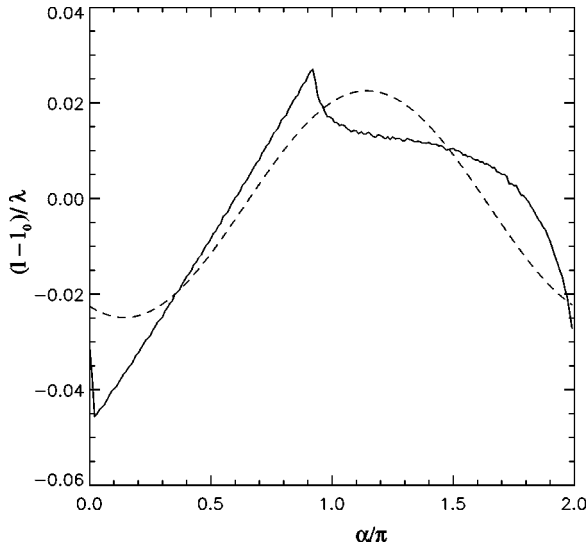


FIG. 5. The shape of the feedback signal $l - l_0$ computed as a function of a rotation angle α (solid line) and its first Fourier harmonic (dashed line). The domain radius $R_d = 1.5\lambda$. Displacement $d = \lambda$.

order to analyze the feedback signal in this regime, the case of an arbitrary large displacement $d < R_d$ should be examined. In contrast to the case of a small displacement, an analytical consideration leads to rather complicated expressions. However, the arc length of an Archimedean spiral within a circular domain can be easily determined numerically.

To perform these computations we assume again that the Archimedean spiral is motionless, while the domain center is displaced initially in the negative x direction and then rotates in accordance with Eq. (10). For numerical procedure it is useful to present a spiral as a sequence of short segments. Then, to estimate the arc length, it is enough to compute a total length of all segments located inside the circular domain. As in the previous case it is assumed that the integral $B(t)$ will be proportional to the arc length $L(t)$ of the spiral inside the rotating domain: $B(t)/b = L(t)/S = l(t)$.

Obviously, $l(t)$ is a periodic function of time, as well as the feedback signal shown in Fig. 3(b) and corresponding to the resonance attractor. Variations of $l(t) - l_0$ during one period are shown in Fig. 5 as a function of the rotation angle α . Obviously, this function is not necessary a simple harmonic one, as it was in the case of a small displacement d [see Eq. (15)]. Nevertheless, it has been shown that only the first component in the Fourier series of a weak periodic forcing can produce a detectable resonant drift [20]. Hence, in order to determine the drift velocity, one has to apply the Fourier expansion to the feedback signal shown in Fig. 5.

In order to be consistent with the previous consideration, let us expand the computed function $l(t) - l_0$ (here $l_0 = L_0/S$) in the following form:

$$l(t) - l_0 = A_0 + A \cos(\omega t - \phi) \quad (26)$$

and skip all other terms like $A_n \cos(n\omega t + \phi_n)$ with $n > 1$. The coefficients in this expansion are

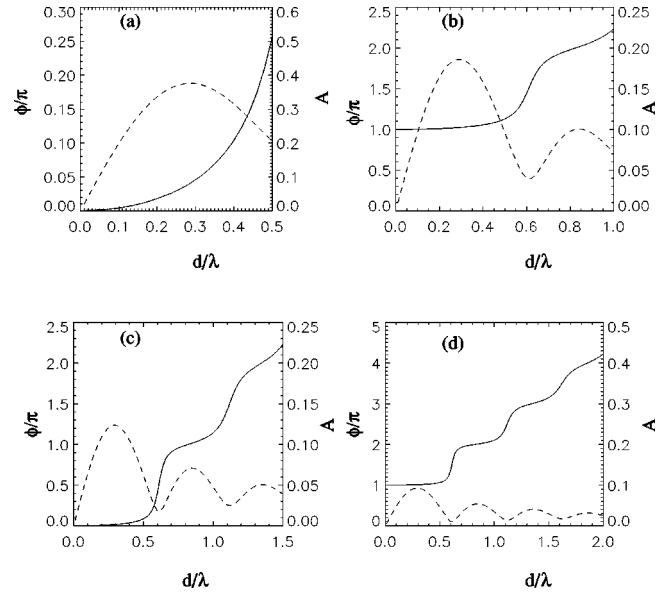


FIG. 6. The phase ϕ (solid line) and the amplitude A (dashed line) of the first Fourier harmonic of the feedback signal $l - l_0$ computed as a function of the displacement d for domains of different radii: (a) $R_d = 0.5\lambda$, (b) $R_d = \lambda$, (c) $R_d = 1.5\lambda$, (d) $R_d = 2.0\lambda$.

$$A_0 = \frac{1}{2\pi} \int_0^{2\pi} [l(\alpha) - l_0] d\alpha,$$

$$A = \sqrt{A_1^2 + B_1^2},$$

$$\phi = \arctan(B_1/A_1),$$

where

$$A_1 = \frac{1}{4\pi} \int_0^{2\pi} [l(\alpha) - l_0] \cos(\alpha) d\alpha,$$

$$B_1 = \frac{1}{4\pi} \int_0^{2\pi} [l(\alpha) - l_0] \sin(\alpha) d\alpha.$$

It is clear that the coefficients A_0, A , and ϕ should depend on two parameters: R_d and d . Figure 6 shows the computed dependencies of ϕ on d/λ for four different values of R_d . The value A_0 remains always relatively small and does not play any important role in the induced drift. The amplitude A vanishes for $d=0$ and for small d linear dependence (16) is valid. Interestingly, $A(d)$ is a nonmonotonous but bounded function of d with a global maximum inversely proportional to R_d . The amplitude A determines the absolute value of the drift velocity.

Most important for the analysis below is the computed value of the phase shift $\phi = \phi(d)$. For small d , ϕ practically does not depend on d , but increases with R_d [cf. Eq. (16)]. For any given R_d , the phase shift grows with d , while the derivative of this increasing function with respect to d oscillates.

As mentioned before, the phase shift in the feedback signal determines the direction of the induced resonant drift.

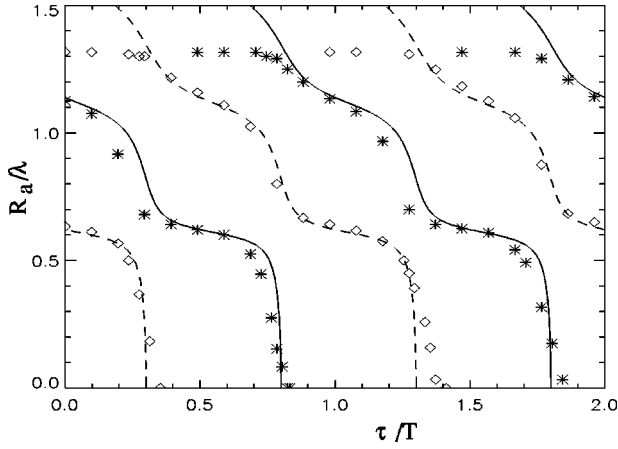


FIG. 7. The radius R_a of the resonance attractor as a function of the time delay τ computed from Eq. (30) for a positive gain (dashed line) and from Eq. (31) for a negative gain (solid line). Computational data obtained after integration of the model (1) are shown as diamonds (asterisks) for the gain $k_{fb}=0.1$ ($k_{fb}=-0.1$). The domain radius $R_d=1.5\lambda$.

Indeed, using the expansion (26) and Eq. (3), the expression for the first harmonic in the feedback signal in the case, when a spiral core center is located at a distance R_c from the domain center, can be written as

$$I(t) = k_{fb} b A(R_c) \cos[\omega t - \omega \tau - \phi(R_c)]. \quad (27)$$

The total phase shift in the feedback signal is the sum $\omega \tau + \phi(R_c)$. In the absence of this shift the spiral wave displaced in the positive x direction will be forced by a signal $I(t) = k_{fb} b A(R_c) \cos(\omega t)$. In accordance with our computations, such a forcing will induce a drift specified by an angle φ with respect to the x axis, as shown in Fig. 1. In the case of an arbitrary displacement R_c the angle γ in Eqs. (19) and (20) can be written as

$$\gamma = \varphi + \omega \tau + \phi(R_c). \quad (28)$$

The necessary condition for the existence of a resonance attractor is a drift in a direction orthogonal to the radial displacement of a spiral wave. Only in the case, when the radial component of the drift velocity is equal to zero, the spiral wave core will describe a circular trajectory around the domain center. In accordance with Eqs. (19) and (28), the necessary condition for the existence of a resonance attractor of radius R_a is

$$\omega \tau + \phi(R_a) = 0.5\pi - \varphi + 2\pi m. \quad (29)$$

This equation is very important, because it allows us to express the attractor radius R_a as a function of the time delay τ using the parametric representation

$$R_a = d, \quad (30)$$

$$\frac{\tau}{T} = 0.25 - \frac{\varphi}{2\pi} - \frac{\phi(d)}{2\pi} + m.$$

Figure 7 shows the function $R_a = R_a(\tau)$ determined for the

domain radius $R_d = 1.5\lambda$. To plot this function, the dependence $\phi(d)$ shown in Fig. 6(c) was used. The dashed curve in the lower left corner corresponds to $m=0$. To obtain the next two dashed curves the values $m=1$ and $m=2$ have been used.

Note that Eq. (30) determines the attractor radius for the case of a positive gain k_{fb} in the feedback loop. A change of the gain sign can be considered as an additional phase shift equal to π . Hence, the attractor radius for a negative gain can be expressed in the following way:

$$R_a = d,$$

$$\frac{\tau}{T} = 0.75 - \frac{\varphi}{2\pi} - \frac{\phi(d)}{2\pi} + m. \quad (31)$$

In Fig. 7 three branches of this dependence corresponding to $m=0,1,2$ are shown by solid curves.

In order to explain why a circular pathway around the domain center plays the role of an attractor of spiral waves, one should consider the corresponding transient process using similar arguments about the drift direction. For instance, in computations illustrated in Fig. 2(b) the spiral wave is initially located rather close to the domain center. The phase shift $\omega \tau + \phi(R_c)$ is small in the generated feedback signal, because $\tau=0$ and $\phi(R_c)$ is negligible [see Fig. 6(c)]. Due to this, the drift initially occurs practically at the angle φ with respect to the radial direction. An increase of R_c results in a growth of the phase shift $\phi(R_c)$ that leads to a rotation of the drift direction to the left. When R_c becomes equal to R_a , the radial component of the drift velocity vanishes and the spiral core starts to describe a circular pathway, corresponding to the resonance attractor. If the distance toward the domain center is suddenly increased due to some fluctuation, a negative component of the radial drift appears, since the phase shift $\phi(R_c)$ grows. This negative radial velocity begins to compensate for the initial fluctuation.

This kinematical consideration can be easily complemented by a linear stability analysis of Eqs. (19) and (28), which should take into account that $\phi(d)$ is an increasing function (see Fig. 6). Stable fixed points of this system correspond to $\gamma = 0.5\pi + 2\pi m$, which leads to Eq. (29). Unstable fixed points are given by $\gamma = -0.5\pi + 2\pi m$ and correspond to separatrices restricting basins of attraction of stable fixed points.

Thus, the existence and stability of the resonance attractor obtain a transparent explanation analyzing of the phase shift in the feedback signal.

VII. COMPARISON WITH COMPUTATIONAL RESULTS

It is important to compare the results of the theoretical analysis with computations performed with the reaction-diffusion model (1). To this aim a number of computations have been performed using different values of the time delay τ and different signs of the gain k_{fb} in the feedback loop. The computed radii of the corresponding resonance attractors are shown in Fig. 7 as separate diamonds and asterisks.

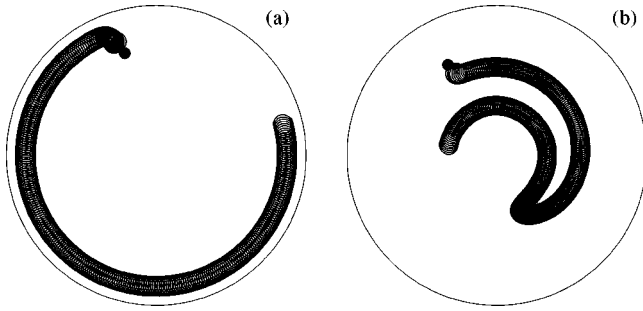


FIG. 8. Trajectory of the spiral wave tip corresponding to the resonance attractor computed for the model (1) with the domain radius $R_d = 1.5\lambda$, the gain $k_{fb} = -0.1$, and the time delay $\tau = 36$. The initial location of the spiral wave tip is shown by the black dot. (a) A long trip the spiral wave corresponds to the resonance attractor under a strong influence of the domain boundary ($0 \leq t \leq 15\,000$). (b) After a long trip along an unstable trajectory the spiral core approaches a stable circular orbit ($0 \leq t \leq 15\,000$).

The computed data agree very well with the theoretical predictions everywhere, except in the region of relatively large R_a . A more detailed consideration of this effect shows that the reason for this discrepancy is a boundary influence. Figure 8(a) shows a characteristic example of a resonance attractor of such a large radius. The performed theoretical consideration did not take into account that a real spiral wave has a core with radius $R_q = 0.092\lambda$. Hence, the attractor radius in reality cannot be larger than $R_d - R_q$. Moreover, the spiral wave cannot survive near the boundary if the core boundary is located directly at the boundary of the domain. A gap with a width about the core radius should be there. Finally, due to the boundary effects the attractor radius cannot be larger than $R_d - 2R_q = 1.42\lambda$. This estimate corresponds very nicely to the upper boundary of the computed attractor radius.

Note that the drift of a spiral wave in a vicinity of the domain boundary becomes extremely sensitive to any disturbances. Only very accurate computations exhibit a long-lasting drift. Any small deviations of the core position directed toward the domain boundary lead to the disappearance of the spiral.

In accordance with Fig. 7, it is possible to have several different resonance attractors for given parameters in the feedback loop. What kind of attractors will be achieved depends, of course, on the initial location of the spiral core. Thus, there should be a separatrix bounding the basin of attraction. It is easy to see that the separatrices for the case of a positive gain k_{fb} obey Eq. (31) describing attractor radii for a negative gain, and vice versa.

A spiral wave initially located exactly on this separatrix can perform a long drift describing this unstable circular pathway, as shown in Fig. 8(b). However, finally the direction of the drift will be changed and it will achieve a stable resonant attractor.

This complicated transient process can be simulated by the system of Eqs. (19), (20), and (28). Note that initially $\gamma \approx -\pi/2$ since the spiral core is located near a separatrix. In accordance with Eq. (20), $d\theta/dt < 0$ and the drift occurs in the clockwise direction. That is a common property of un-

stable orbits: the drift direction is opposite to the rotation direction of a spiral. Decrease of R_c during the drift induces further decrease of γ first until $\gamma = -\pi$ (the azimuthal drift vanishes at this instant) and then until $\gamma = -1.5\pi$ which corresponds to a stable orbit. For all attractors the induced rotation of the spiral core coincides with the rotation direction of a spiral wave.

The performed computations allow us also to verify the theoretical predictions about the stability of the centrally symmetric rotation of spiral waves. To this aim, taking into account that in the model $\phi = -0.1$, Eq. (22) can be written as

$$0.3 + m < \tau/T < 0.8 + m. \quad (32)$$

These inequalities determine intervals of the τ/T axis in Fig. 7 locating between dashed (left boundary) and solid (right boundary) curves. Our computations indeed demonstrate the existence of the centrally symmetric rotation (i.e., the resonance attractor with $R_a = 0$) in the predicted regions, except for small deviations of the boundaries specified by inequalities (32).

The drift velocity is another important characteristic of the resonance attractor. One can assume that for slow drift its velocity is proportional to the amplitude of the feedback signal. In all our computations the absolute value of the gain k_{fb} in the feedback loop was the same: $|k_{fb}| = 0.1$. However, the amplitude A of the generated feedback signal depends on the displacement d from the domain center, as shown in Fig. 6(c). The small value of the amplitude A at $d = 0.6\lambda$ explains the extremely slow drift velocity for the attractor shown in Fig. 2(b). In contrast to this, the drift velocity for the attractor shown in Fig. 2(c) is relatively fast, because the function $A(d)$ achieves a maximum near $d = 0.3\lambda$.

The predicted drift velocity does not depend on the gain sign and on the time delay τ . It depends on the absolute value of the gain k_{fb} and on the attractor radius R_a . In accordance with this, the drift velocity is also very small for $R_a \approx 0.6\lambda$ in the computations shown in Fig. 8(b).

The domain radius is another important factor that influences the drift velocity. As mentioned before, the amplitude of the first Fourier component is inversely proportional to R_d as it can be seen in Fig. 6. To compensate for this decreasing of the drift velocity it is possible to increase the gain k_{fb} in the feedback loop. However, there are many restrictions, for instance, an enhancement of computational noise, which do not allow us to apply infinitely large gain. Thus, one can expect extremely slow drift if $R_d \gg \lambda$.

Thus, the predicted direction and the absolute value of the induced drift, the attractor radius and the regions of the centrally symmetrical rotation are in very good agreement with computations performed on the reaction-diffusion model.

VIII. CONCLUSION

Our computations demonstrate the existence of the resonance attractors of spiral waves rotating in an excitable medium under global feedback. The theory of the resonance attractor in a circular domain developed in this work is based

on the finding that the direction of the drift induced by the global feedback can be specified as a function of the spiral core location and does not depend on the initial orientation of the spiral wave. This theory explains the phenomena of stabilization and destabilization of the centrally symmetric rotation of spiral waves for the domains of different sizes and predicts the existence of attractors with different radii. It allows us to explain the attractor stability and gives quantitative expressions of the attractor radius as a function of the domain size and of the time delay in the feedback loop.

The only quantity that should be measured in order to apply these theoretical predictions is the angle φ that specifies the direction of a resonant drift (see Fig. 1). Thus, the obtained theoretical results can be easily checked experimentally. The light-sensitive Belousov-Zhabotinsky reaction is probably the most convenient object for such experimental verification, although spiral waves are effectively studied in context of CO oxidation on platinum surface [24] and excitation waves in cardiac tissue [25], too.

The obtained quantitative expressions are based on the assumptions that a rigidly rotating spiral wave has an Archimedean shape and the velocity of the induced drift is small. These conditions are fulfilled for a spiral in media with a low excitability independent of their physical nature. Hence, the application field of the elaborated theory is very broad. For instance, in the framework of this theory the stabilization and destabilization of the centrally symmetric rotation in a circular domain discovered in recent computations [15] obtain a

clear explanation. Also the experimental observations of the resonance attractor under feedback derived from a confined circular domain [26,27] can be quantitatively explained.

Spiral wave dynamics under global feedback constitutes a broad and prospective field for both theoretical and experimental studies. Only a very symmetrical case of a circular domain has been considered in this paper. It is clear that small deviation from this shape cannot change the main properties of the observed drift unless they do not change the first Fourier component of the feedback signal. However, an essential variation of the domain geometry (to square or ellipse) can induce some additional properties of the spiral wave dynamics. Interesting challenges for future work can be also the investigation of the influence of the global feedback on a meandering spiral or the transition to a large gain in the feedback loop. Both of these aspects are very important for such applications as the defibrillation of cardiac muscle. From the theoretical point of view it is very interesting to clarify a correspondence between the resonance attractor under global and one-channel feedback. To this aim one should bring together two quite different theoretical approaches.

ACKNOWLEDGMENTS

The authors thank the Deutsche Forschungsgemeinschaft (DFG, SFB 555) for financial support.

-
- [1] K. Hall, D.J. Christini, M. Tremblay, J.J. Collins, L. Glass, and J. Billette, *Phys. Rev. Lett.* **78**, 4518 (1997).
- [2] E.V. Nikolaev, V.N. Biktashev, and A. Holden, *Chaos, Solitons Fractals* **9**, 363 (1998).
- [3] A.V. Panfilov, S.C. Müller, V.S. Zykov, and J.P. Keener, *Phys. Rev. E* **61**, 4644 (2000).
- [4] S. Grill, V.S. Zykov, and S.C. Müller, *Phys. Rev. Lett.* **75**, 3368 (1995).
- [5] S. Grill, V.S. Zykov, and S.C. Müller, *J. Phys. Chem.* **100**, 19 082 (1996).
- [6] A. Karma and V.S. Zykov, *Phys. Rev. Lett.* **83**, 2453 (1999).
- [7] M. Braune and H. Engel, *Phys. Rev. E* **62**, 5986 (2000).
- [8] O.U. Kheowan, V.S. Zykov, O. Rangsiman, and S.C. Müller, *Phys. Rev. Lett.* **86**, 2170 (2001).
- [9] V.S. Zykov, O.U. Kheowan, O. Rangsiman, and S.C. Müller, *Phys. Rev. E* **65**, 026206 (2002).
- [10] K.I. Agladze, V.A. Davydov, and A.S. Mikhailov, *Pisma Zh. Eksp. Teor. Fiz.* **45**, 601 (1987) [*JETP Lett.* **45**, 767 (1987)].
- [11] O. Steinbock, V.S. Zykov, and S.C. Müller, *Nature (London)* **366**, 322 (1993).
- [12] M. Braune and H. Engel, *Chem. Phys. Lett.* **211**, 534 (1993).
- [13] M. Falcke, H. Engel, and M. Neufeld, *Phys. Rev. E* **52**, 763 (1995).
- [14] M. Kim, M. Bertram, M. Pollman, A. von Oertzen, A.S. Mikhailov, H.H. Rotermund, and G. Ertl, *Science* **292**, 1351 (2001).
- [15] V.S. Zykov, A.S. Mikhailov, and S.C. Müller, *Phys. Rev. Lett.* **78**, 3398 (1997).
- [16] V.S. Zykov, *Simulation of Wave Processes in Excitable Media* (Manchester University Press, Manchester, 1987).
- [17] N. Wiener and A. Rosenblueth, *Arch. Inst. Cardiol. Mex* **16**, 205 (1946).
- [18] A.T. Winfree, *Science* **175**, 634 (1972).
- [19] V.A. Davydov, V.S. Zykov, and A.S. Mikhailov, *Usp. Fiz. Nauk* **161**, 45 (1991) [*Sov. Phys. Usp.* **34**, 665 (1991)].
- [20] R.M. Mantel and D. Barkley, *Phys. Rev. E* **54**, 4791 (1996).
- [21] V.S. Zykov, O. Steinbock, and S.C. Müller, *Chaos* **4**, 509 (1994).
- [22] A. Schrader, M. Braune, and H. Engel, *Phys. Rev. E* **52**, 98 (1995).
- [23] N. Gottschalk, M. Hildebrand, M. Bär, and M. Eiswirth, *Phys. Rev. E* **52**, R5731 (1995).
- [24] S. Jakubith, H.H. Rotermund, W. Engel, A. von Oertzen, and G. Ertl, *Phys. Rev. Lett.* **65**, 3013 (1990).
- [25] J.M. Davidenko, A.V. Pertsov, R. Salomonsz, W. Baxter, and J. Jalife, *Nature (London)* **355**, 349 (1992).
- [26] O. Kheowan, C.K. Chan, V.S. Zykov, O. Rangsiman, and S.C. Müller, *Phys. Rev. E* **64**, 035201(R) (2001).
- [27] O.U. Kheowan, V.S. Zykov, and S.C. Müller, *Phys. Chem. Chem. Phys.* **4**, 1334 (2002).